Journal Pre-proof

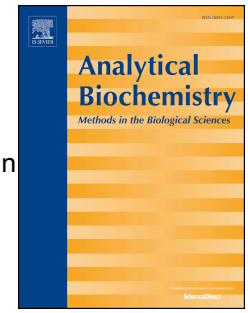

Inhibitor screening assay for neurexin-LRRTM adhesion protein interaction involved in synaptic maintenance and neurological disorders

Sudeep Karki, Mirko M. Maksimainen, Lari Lehtiö, Tommi Kajander

PII: S0003-2697(19)30607-4

DOI: https://doi.org/10.1016/j.ab.2019.113463

Reference: YABIO 113463

To appear in: *Analytical Biochemistry*

Received Date: 24 June 2019

Revised Date: 26 September 2019

Accepted Date: 26 September 2019

Please cite this article as: S. Karki, M.M. Maksimainen, L. Lehtiö, T. Kajander, Inhibitor screening assay for neurexin-LRRTM adhesion protein interaction involved in synaptic maintenance and neurological disorders, *Analytical Biochemistry* (2019), doi: https://doi.org/10.1016/j.ab.2019.113463.

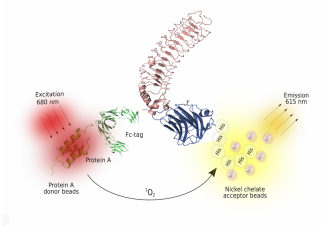

Inhibitor screening assay for neurexin-LRRTM adhesion protein interaction involved in synaptic maintenance and neurological disorders

Sudeep Karki[1], Mirko M. Maksimainen[2], Lari Lehtiö[2] and Tommi Kajander*[1]

[1]Institute of Biotechnology, University of Helsinki, Finland

[2] Faculty of Biochemistry and Molecular Medicine and Biocenter Oulu
University of Oulu, Finland

*****Corresponding author: tommi.kajander@helsinki.fi

Tommi Kajander

Institute of Biotechnology

Viikinkaari 1 (PO Box 65)

University of Helsinki

00014 Helsinki

Subject category: Membranes and receptors

Keywords: AlphaScreen, in-cell western blot, LRRTM, neurexin, synapse, adhesion, inhibitor assay, neurological disorders

Abstract

Synaptic adhesion molecules, including presynaptic neurexins (NRXNs) and post-synaptic leucine-rich repeat transmembrane (LRRTM) proteins are important for development and maintenance of brain neuronal networks. NRXNs are probably the best characterized synaptic adhesion molecules, and one of the major presynaptic organizer proteins. The LRRTMs were found as ligands for NRXNs. Many of the synaptic adhesion proteins have been linked to neurological cognitive disorders, such as schizophrenia and autism spectrum disorders, making them targets of interest for both biological studies, and towards drug development. Therefore, we decided to develop a screening method to target the adhesion proteins, here the LRRTM-NRXN interaction, to find small molecule probes for further studies in cellular settings. To our knowledge, no potent small molecule compounds against the neuronal synaptic adhesion proteins are available. We utilized the AlphaScreen technology, and developed an assay targeting the NRXN-LRRTM2 interaction. We carried out screening of 2000 compounds and identified hits with moderate IC_{50}-values. We also established an orthogonal in-cell western blot assay to validate hits. This paves way for future development of specific high affinity compounds by further high throughput screening of larger compound libraries using the methods established here. The method could also be applied to screening other NRXN-ligand interactions.

1. Introduction

The synaptic adhesion molecules such as presynaptic neurexins (NRXNs) and post-synaptic leucine-rich repeat (LRR) proteins including the LRR transmembrane (LRRTM) family of proteins are important for the development and maintenance of brain and formation of neuronal networks. Synapses are the major contact and information relay points between the individual neurons that constitute the neuronal network of the brain [1, 2]. NRXNs are probably the best characterized synaptic adhesion molecules [3, 4, 5, 6] and one of the major presynaptic organizer proteins [7].

Mammals have three NRXN genes (NRXN1-3), and each NRXN gene produces two isoforms, NRXNα and NRXNβ. In addition, NRXNs can produce potentially thousands of different splice variants [6]. The NRXNαs have five canonical splice sites, SS1-SS5, of which SS4 and SS5 are also present in the NRXNβ genes [3]. The NRXN interactions are largely Ca^{2+} dependent [3]. They have several post-synaptic ligands such as neuroligins [8], LRRTMs[4], neuroxophilin, dystroglycan [9], cerebellin [10] and calsyntenins [11]. The NRXNs and LRRTM interaction requires the splice form lacking the SS4 splice site sequence [12]. NRXNs family proteins are found in both excitatory and inhibitory synapses. The extracellular part of NRXNs constitutes of LNS (laminin, NRXN and sex-hormone-binding protein) and EGF domains. NRXNα has 6 LNS domains (L1-6), arranged in three modules with EGF domains (E1-3) between two LNS domains (Fig. 1A). NRXNβ contains only one LNS-domain, identical to the NRXN-α LNS6, after which there is a highly glycosylated linker region and a transmembrane (TM) domain and an intracellular tail with a PDZ binding motif, that interacts with the presynaptic organizing machinery [3]. Structures of both partial NRXNα ectodomain and various NRXNβ constructs alone and in complex with neuroligin ligands have been resolved by X-ray crystallography [13, 14, 15, 16] .

The LRRTM family of proteins that include four members are found in the excitatory glutamatergic synapses of the brain and were found originally as ligands of NRXNs [17, 18, 19]. LRRTMs all share the same domain organization with N-terminal extracellular domain with ten repeat LRR domain followed by a linker region and TM domain, and intracellular tail with a PDZ binding motif (Fig. 1A) anchoring the LRRTMs to post-synaptic density organizing proteins and the glutamate receptors. We have earlier solved the structure of engineered thermostabilized LRRTM2 extracellular domain [20] and recently the LRRTM2-NRXNβ1 complex crystal structure was solved [21], revealing the interaction interface, located surprisingly in the helical C-

terminal capping region of the LRR domain on LRRTM2 (Fig. 1B). Further, in particular LRRTM4, but probably also other LRRTMs, have also been found to be ligands for heparan sulphate proteoglycans [18, 22]. It has been suggested that NRXNs are post-translationally decorated with heparan sulphate in the membrane proximal region of the extracellular domain and this might increase the affinity towards LRRTMs [23]. Other ligands are currently not known for LRRTMs, and thus their ligand repertoire is not as wide as for NRXNs.

Many of the synaptic adhesion proteins have been genetically linked to neuronal disorders, in particular, cognitive disorders such as schizophrenia, autism spectrum disorders and bipolar disorder [24, 25], which make them targets of interest for biological, therapeutic and disease mechanism studies in model organisms or in cell culture. For the functional studies of synaptic adhesion proteins, both gain-of-function and loss-of-function studies have been important. However, overall loss-of-function studies would benefit from specific compounds that target a particular interaction, e.g. studies with knock-out animals or neuronal cultures would be potential applications for such effector molecules. Loss-of-function studies have involved generation of knock-down and knock-out mice for various adhesion proteins. For NRXNs, neuroligins and LRRTMs it has been shown that single knock-downs are not necessarily lethal and probably single knock-downs can be compensated functionally by the other homologs or ligands to some extent [17], while triple NRXNα knock-outs are lethal [26, 27]. Currently, no inhibitor compounds for these synaptic adhesion proteins are available to our knowledge. Therefore, we have taken up the task to develop a screening method to target adhesion protein interactions, here, the LRRTM-NRXN interaction. We utilized the AlphaScreen technology[28] (Fig. 1B) and developed an assay for screening compounds targeting the LRRTM-NRXN interaction. We carried out validatory screening and identified several hits with moderate IC_{50}-values in the range of tens of micromolar. We also established and used an orthogonal assay to validate the potency of the hits in a cell-based assay. This setup paves way for the future development of specific high-affinity compounds either through optimization of the obtained hit compounds or by further high throughput screening of larger compound libraries using the methods established here.

2. Materials and methods

2.1 Cloning, protein expression and purification

Extracellular regions of the mouse LRRTM2 ($LRRTM2_{30-421}$) and NRXNα1 ($NRXN\alpha1_{31-1286}$, lacking the SS4 splice site) were cloned into *Drosophila* pRMHA3 expression vector [29]. The expression constructs included a CD33 signal sequence at the N-terminus of the insert and a C-terminal Fc-tag. LRRTM2-Fc was expressed from stably transfected *Drosophila* S2 cells, and expressed and purified as described previously [20].

NRXNα1-Fc protein construct was expressed from stably transfected *Drosophila* S2 cells. Expression was verified by transient transfection using western blot method with goat polyclonal horse radish peroxidase (HRP) conjugated antibody (Abcam, ab98567) against human IgG-Fc. For expression from stable cell line of S2 cells, 1.25×10^6 cells per well were plated on a six-well plate at room temperature. After 24 hours, the cells were transfected with 4 µg of DNA containing 1:20 part of selection plasmid pCoHygro. The DNA was diluted into 400 µL of the medium; 8 µL of TransIT insect reagent (Mirus Bio LLC) was mixed with the DNA, and the mixture was incubated for 20 min and added to the cells. After 3 days, the selection was started; the cells and medium were centrifuged and the cells were resuspended into medium with 0.3 mg/mL hygromycin and re-plated into the same wells. After 3 weeks, the cells were grown in T75 flask (ThermoFischer). The cells were passaged every 6 days in T75 flask until the cell viability was above 95%. For large scale purification from the generated stable cell line, the S2 cells were diluted 1:10 into HyQ-SFX (ThermoFischer) medium supplemented with 0.15 mg/mL hygromycin, grown in shaker at 25°C for 1 day, and induced with 0.7 mM CuSO4, and expression was conducted for further 6 days, after which the medium was harvested and cells were pelleted by centrifugation at 7000 rpm for 20 min at 4°C. The protein was purified using the C-terminal Fc-fusion tag with protein-A sepharose (Invitrogen). Samples were eluted with 0.1 M glycine (pH 3.0) directly to neutralizing buffer, 60 mM Tris (pH 7.4), 300 mM NaCl.

The NRXNβ1 gene construct (His_6-$NRXN\beta1_{40–216}$ LNS domain lacking the SS4 splice site sequence) was cloned into pHYRSF53LA vector. The resulting His-NRXNβ1 construct was expressed from *E. coli* BL21(DE3) in LB medium at 37 °C and induced at an OD_{600} of 0.8 with 1 mM IPTG, and expressed for 4–5 h at 30 °C, after which the cells were collected and suspended in 50 mM Tris HCL pH8, 300 mM NaCl. Cells were lysed via sonication. The His_6-tagged NRXNβ was purified with HisTrap™ column (GE Healthcare) and eluted with 50 mM Tris HCl pH 8, 300 mM NaCl, 250 mM imidazole. The protein was further purified with size exclusion chromatography with S-75 Superdex 10/300 column (GE Healthcare) in 30 mM Tris pH 7.5 and 300 mM NaCl.

The Fc-His_6-pETDuest plasmid was expressed from *E. coli* BL21(DE3) in LB media at 37 °C and induced at an OD_{600} of 0.6 with 1 mM IPTG, and expressed for 4 hours at 30 °C, after which the cells were collected and suspended in 20 mM sodium phosphate pH 8.0, 150 mM NaCl, and 10 mM imidazole buffer. Cells were lysed via sonication and supernatant collected, and Fc-His_6 protein was purified with Ni^{2+}-NTA resin (Qiagen), further purification by size exclusion chromatography was done with S-200 Superdex 10/300 column in 1x PBS buffer.

2.2 Assay Development

We utilized the AlphaScreen technology [28] to develop a binding assay to screen inhibitors for the LRRTM2-NRXN interaction. All AlphaScreen assays were performed using AlphaPlate384 (PerkinElmer) plates. The AlphaScreen reaction consisted of LRRTM2-Fc, His-NRXNβ1, Protein A donor and nickel chelate acceptor beads (PerkinElmer) (Fig. 1B) in assay buffer containing 30 mM HEPES (pH 7.5), 150 mM NaCl, 1 mg/mL bovine serum albumin (BSA) and 0.2 mM $CaCl_2$. The plates were incubated at room temperature and protected from light after addition of the AlphaScreen beads. Luminescence was monitored with Tecan infinite M1000 Pro plate reader using the AlphaScreen detection module with 100 ms excitation and 300 ms integration times.

Assay sensitivity was first tested in order to establish the optimal concentrations of LRRTM2-Fc and His-NRXNβ1, and to obtain a maximal AlphaScreen signal (hook point). A reaction mixture of LRRTM2-Fc and His-NRXNβ1 was prepared in a total volume of 15 µl, followed by incubation at room temperature for 2 hours. After the incubation, the AlphaScreen beads were added according to the recommended protocol (PerkinElmer): first 5 µl of the acceptor beads were added, followed by 30 min of incubation and addition of 5 µl of the donor beads, followed by 60 min incubation. The final concentrations of LRRTM2-Fc and His-NRXNβ1 were 0-0.5 µM, and 50 µg/ml of the acceptor and donor beads.

2.3 Assay optimization

After assay development, we optimized different assay parameters that included protein incubation time, order of addition of beads, bead concentration and bead incubation time. First, we optimized the incubation time for the interaction of LRRTM2-Fc and His-NRXNβ1 by testing different times from 5 minutes to 2 hours. Second, the order of addition of the beads was determined with three sequences, (a) both beads were added together, followed by 90 min of incubation; (b) the acceptor beads were added and incubated for 30 min, followed by addition of the donor beads and addition

incubation for 60 min, and (c) the donor beads were added and incubated for 30 min, followed by addition of the acceptor beads and addition incubation for 60 min. Third, the concentration and incubation times of the beads was optimized by testing different concentrations: 20, 10, 5 and 2.5 µg/ml and incubation times from 60 minutes to 7 hours. Finally, we measured the DMSO tolerance of the assay in the 0–10% DMSO concentration range.

Ethylene glycol-bis(2-aminoethylether)-N,N,N',N'-tetra acetic acid (EGTA) was tested as a positive control to inhibit the LRRTM2-NRXN interaction. We measured the effect of 100 µM - 1 mM EGTA on the interaction using the selected final assay conditions. For the validation, we also tested if EGTA in the range of 50 nM to 5 mM is able to quench the AlphaScreen signal. For this we used the commercial AlphaScreen Biotinylated-His peptide assay (PerkinElmer).

2.4 Assay validation

We validated the assay by measuring the repeatability of the maximal and minimal signals between different plates, wells and days. Altogether during 3 days, we measured five plates containing maximal and minimal signals; one plate on days 1 and 2, and three plates on day 3. Each plate included forty maximal and minimal signal points. Variations of well-to-well, plate-to-plate, and day-to-day were calculated as coefficients of variations (CVs). The quality of the data was measured with common statistical parameters: signal-to-noise ratio (S/N), signal-to background-ratio (S/B), and screening window coefficients (Z') [30, 31].

2.5 Library and counter screening

We screened MicroSource Spectrum compound library with 2000 compounds (obtained from FIMM, University of Helsinki) at a single concentration (100 µM). 250 nl of 10 mM compounds were transferred to the assay plates with Labcyte Echo 550 acoustic dispenser. 15 µl of the mixture of 50 nM LRRTM2-Fc and 50 nM His-NRXNβ1was added to the assay plates. The plates were incubated for 5 minutes at room temperature, followed by addition of acceptor and donor bead mixture (10 µl, final concentration of 5 µg/ml) according to the optimized procedure, and incubated further at room temperature for 3 hours. Each screening plate contained blank wells (AlphaScreen beads only), positive controls (inhibition by 0.2 mM EGTA) and negative controls (0% inhibition; no EGTA or added compounds).

The counter screening assay was performed in order to rule out false positives obtained from the library screening. For this we used Fc-His_6 protein, which binds both donor and acceptor beads

creating an AlphaScreen signal. Compounds decreasing the signal are considered as false-positives due to interaction with the beads or quenching the signal. We performed the counter screening using 100 µM compound concentration. 15 µl of 16.5 nM Fc-His_6 in 25 mM HEPES pH 7.5, 150 mM NaCl, 1 mg/ml BSA was added to plate wells followed by addition of 10 µl of AlphaScreen bead mixture containing 5 µg/ml of the acceptor and donor beads. The plate was incubated at room temperature for 3 hours before reading.

2.6 Potency Measurement

Concentration response curves for the hit compounds were measured in quadruplicates from 300 µM to 1 µM using quarter-logarithmic dilutions. The compounds were transferred to the assay plate using Labcyte Echo 550 acoustic dispenser, followed by addition of 15 µl of the mixture of 50 nM LRRTM2-Fc and 50 nM His-NRXNβ1. The plates were incubated for 5 minutes at room temperature, followed by addition of 10 µl of acceptor and donor bead mixture (final concentration 5 µg/ml) and an additional incubation at room temperature for 3 hours. The dose-response curves were fitted using a four-parameter nonlinear regression analysis (sigmoidal dose-response fitting with variable slope) with GraphPad Prism version 5.03 for Windows (GraphPad Software).

2.7 Cell culture and cell-based binding assay

For cell-based binding assays, we used the mouse LRRTM2 cDNA cloned into pEGFP-N1 plasmid vector [20]. We employed the in-cell western blot method to detect the LRRTM2-NRXNα1 interaction on cell surface with the Odyssey Infrared Imaging System (LI-COR Biosciences) following manufacturer's recommendations. In this assay LRRTM2 was expressed in HEK293T cells as a C-terminal GFP-fusion to enable visualization of the protein expression on 96-well cell culture plates. The soluble NRXNα1-Fc was added on the cells in a 96-well plate and binding was detected with anti-human Fc antibody and signal per well was read with the Odyssey Imaging system.

For the transfection of LRRTM2-pEGFP-N1 into Human embryonic kidney 293T (HEK293T) cells, cells were grown to 90% confluency on a T75 flask using DMEM media with 10% FBS (ThermoFisher) at 37 °C and 5% CO_2. These cells were washed in 1x PBS and trypsinized in 0.05% Trypsin-EDTA pH 7.4. Cells were seeded into a poly-L lysine-coated 96 well plate at approximately 20 000 cells/well, and they were allowed to grow 24 hours at 37° C until they reached confluency of 90%. After 24 hours, the cells were transfected with LRRTM2-pEGFP-N1 (400 µg/well) plasmid

and polyethylenimine (1.2 µg/well). The transfected cells were incubated at 37° C for 48 hours and preceded for in-cell western blot assay. The LRRTM2-GFP fusion protein expression in transfected cells was detected with Floid™ Cell Imaging system (ThermoFischer). For the in-cell western blot experiment, LRRTM2-pEGFP-N1 transfected cells were washed with 1xPBS and blocked with EGB buffer [22] (168 mM NaCl, 2.6 mM KCl, 10 mM HEPES pH 7.2, 2 mM $CaCl_2$, 2 mM $MgCl_2$, 10 mM D-glucose, and 5% BSA) for 2 hours at room temperature with slow shaking. Blocking buffer was removed and cells were covered in 50 µl of NRXNα1-Fc diluted in EGB buffer with 1% BSA. The cells were incubated overnight at 4° C with gentle shaking. Next day, cells were washed with 1xTBS buffer and were then incubated with 50 µl of 1:200 dilution of secondary antibody (goat anti-human IgG IRDye 800CW) in EGB buffer with 1% BSA. Following a 60 minute incubation at room temperature with gentle shaking, plates were washed with 1xTBS, and further scanned using LI-COR Odyssey (169 µm resolution and medium quality) with channel (800 nm) intensity of 8. For assay development, initially different concentrations of NRXNα1-Fc (10 nM to 1000 nM) were used, and the minimum concentration which gave the saturation signal was used for the in-cell western blot assay of LRRTM2 and NRXNα1-Fc in presence of inhibitor compounds.

Inhibition assay was performed in triplicates (n=3) and each assay was repeated three times. The compounds pyrithione zinc, benzoxiquine, indole-3-carbinol and 6-methoxyharmalan were ordered from Sigma-Aldrich, and iodoquinol, pyrvinium pamoate and econazole nitrate were ordered from MedChemExpress. For inhibition assay, HEK293T cells transfected with LRRTM2-pEGFP-N1 in 96 well plate was washed with 1 x PBS and blocked with EGB buffer with 5% BSA for 2 hours at room temperature. After blocking for 2 hours, 0.8 µM NRXNα1-Fc diluted in EGB buffer with 1% BSA and 300 µM hit compounds were added in each well. Inhibition of the LRRTM2-NRXNα1-Fc interaction was detected using 1:200 dilution of goat anti-human IgG IRDye 800CW secondary antibody and detected with the LI-COR Odyssey Imaging system. As negative controls for the assay we used i) 2 µM purified receptor protein tyrosine phosphatase σ-Fc fusion protein (RPTPσ-Fc) or ii) 1-2 µM purified Fc-fragment added on to the cells, and iii) plain HEK293T-cells without LRRTM2 expression, but with addition of 1 µM NRXNα1-Fc or iv) HEK293T cell expressing LRRTM2 but without soluble ligands added. RPTPσ-Fc was purified as described previously [32].

3. Results

3.1 Binding assay for LRRTM2-NRXN β-1 interaction

In this paper, we have aimed to establish a screening assay for identification of compounds inhibiting trans-synaptic interaction of the postsynaptic LRRTM2 with presynaptic NRXNs. Previously, no such assay has been reported for synaptic adhesion proteins. The assay measures the proximity-generated luminescence using the AlphaScreen technology. An LRRTM2-Fc construct bound to Protein A donor beads, and a His-NRXNβ1 construct lacking the SS4 splice site, binding to the nickel-chelate acceptor beads were used for the assay. The interaction of LRR domain of LRRTM2 with the LNS domain of NRXN brings the protein donor beads close to the acceptor beads, and the proximity of the beads leads to the transfer of energy due to excitation of donor beads, resulting in luminescence emission by acceptor beads at 520-620 nm (AlphaScreen signal, Fig. 1B) [28]. Loss of LRRTM2-NRXNβ1 interaction is read as a decrease of in total luminescence in comparison to the control. The assay sensitivity was first tested to establish the optimal concentrations of LRRTM2-Fc and His-NRXNβ1 to obtain the maximal AlphaScreen signal. This was obtained with 50 nM of LRRTM2-Fc and 50 nM of His-NRXNβ1 (Fig. 2A).

Once we had established the assay, we optimized different assay parameters including protein incubation time, order of addition of donor and acceptor beads, bead concentration and bead incubation time. We first optimized the incubation time for the interaction of LRRTM2-Fc and His-NRXNβ1. No major difference in the AlphaScreen signal was detected with increase in incubation time, therefore we selected the shortest 5 min protein incubation time (Fig. 2B). To increase robustness of the assay, we tested different order of addition of beads (Fig. 2C). Acceptable signal window for screening was obtained after mixing the donor and acceptor beads followed by addition of bead mixture in the reaction mixture containing LRRTM2-Fc and His-NRXNβ1, and further incubation for 90 minutes. In order to decrease the running cost of the assay, we tested different beads concentrations and incubation times, and acceptable signal was detected with 5 µg/mL of the acceptor and donor bead mixture, followed by incubation time of 3 hours (Fig. 2D and 2E). The aim was to achieve robust screening assay with high signal-to-noise ratio, with reduced the running costs. We found the following protocol to be most optimal for the assay in terms of the both robustness and cost-effectiveness: 15 µl of a reaction solution containing 50 nM LRRTM2-Fc and 50 nM of His-NRXNβ1was incubated for 5 minutes, before adding 10 µl of 5 µg/mL the AlphaScreen acceptor and donor bead mixture followed by incubation of 3 hours before signal detection. This would result in approximately 0.15$ costs per well for larger assays (e.g. with tens of thousands of conditions) excluding compound and dispensing costs.

The LRRTM2-NRXN interaction has clearly been shown to be calcium dependent in cell-based assays [3, 17]. Therefore, we tested if we could use the calcium chelator EGTA as a control for inhibition the interaction. Experiments showed that addition of 0.5 mM EGTA decreased the AlphaScreen signal down to ca. 5% indicating loss of the LRRTM2-NRXN interaction at 0.2 mM Ca^{2+}-ion concentration, while initial 2 mM $CaCl_2$ used in the assay was too high to be inhibited (Fig. 2F). It was further verified with Biotinyled-His peptide (Biotinylated-HIS, PerkinElmer) that EGTA did not interfere with the assay itself and EGTA indeed did not quench the AlphaScreen signal at the concentrations used through e.g. Ni-chelation (Fig. 2G).

We also measured the affinity for the LRRTM2-NRXNβ1 interaction with purified soluble proteins by surface plasmon resonance (SPR) in presence of Ca^{2+}, and found it to be similar to that reported recently by others [20], with a K_d-value of 6.6 μM. We further confirmed by SPR that in presence of 2 mM EGTA in the buffer the affinity was lost, as only 2.4% of signal was left at 50 μM NRXNβ1 concentration (Supplementary material, Suppl. Fig. 1).

Next, since DMSO is a commonly used solvent for the compound libraries, we tested the DMSO tolerance of the assay. The assay was found to tolerate DMSO up to the tested 10% concentration. No substantial deviation in signal between control reaction without DMSO and the 10% DMSO containing reaction was found (Fig. 2H).

In order to validate the quality of the assay for screening, we tested the changes in the plate-to-plate and day-to-day minimal and maximal signals with five different plates. The average Z' value for all the plates was 0.82 with high signal-to-noise ratio, indicating that the screening assay was robust (Table 1).

Table 1. Assay performance.

S/B	14.9 ± 0.9
S/N	19.0 ± 4.9
Z'	0.82 ± 0.04
Well to well CV (max/min,%)	5.04 ± 0.98 / 8.35 ± 5.8
Plate to plate CV (%) *	4.7
Day-to-day CV (%)*	4.17 (2.83-6.59)

* Calculated from Z'-values (see text for definitions).

3.2 Screening and potency measurements

We next performed a validatory screening assay using the MicroSource Spectrum library of 2000 compounds, which includes drugs, natural products, and bioactive compounds. The compounds were used at 100 µM concentration. The assay performed well in screening, with an average Z' of 0.8 ± 0.02 over six plates calculated from the control wells. We obtained 92 initial hits with a 4.6% hit-rate, all of which decreased the AlphaScreen signal at least to same extent as EGTA, indicating potential inhibition of LRRTM2-NRXNβ1 interaction (Fig. 3A).

However, as the hit-rate was high due to the high concentration used, and likely due to the nature of the validatory compound library, we also controlled for false positives through counter screening. Possible mechanisms of non-specific interference with the AlphaScreen signal that the compounds could manifest include 1) by acting as singlet oxygen quenchers, 2) by interfering with the production of luminescence signal itself, or 3) binding to the donor or acceptor beads and interfering with the ligand tag (His-tag or Fc-fragment) binding. In order to rule out false positives we performed a counter screen with the initial 92 hits and His-tagged Fc-fragment binding both the donor and acceptor beads in absence of the actual target interactor proteins to monitor for the AlphaScreen signal. From this we obtained 12 hits that did not interfere with the output signal, out of the initial 92 hits (Fig. 3B), 80 compounds thus interfered with the assay and were excluded. These were not analyzed further, but the 12 hit compounds that did not interfere in the counter screen were taken further for validation. The final hit-rate based on the set hit limit after counter screening was thus 0.6%.

Dose-response curves were measured for further validation for the 12 hit compounds (Fig. 4), which revealed four of the initial hits (solasodine, meta-cresyl acetate and harmaline and penicillin) as actual false positives. The IC_{50} values for the remaining eight hit compounds were between 30-76 µM (Fig. 4 & 5). These were further checked for pan-assay interference compounds (PAINS) patterns to recognize possible frequent false hits, and from these early hit compounds only iodoquinol and pyrvium pamoate (Fig. 5) contained recognizable PAINS and aggregation patterns when analysed with the ZINC server (http://zinc15.docking.org/patterns/home/) [33]. Hence, the results on these two compounds should be further validated, in case these compounds are used and developed further.

3.3 Cell binding assay

Next, we performed an in-cell western blot assay to detect the binding affinity of NRXNα1-Fc to LRRTM2 expressed on HEK293T cells in order to use this as an orthogonal assay for the verification of inhibition of binding, as explained in the methods. We measured the apparent binding affinity of soluble dimeric NRXNα1-Fc to LRRTM2 on the cell surface to be 154 ± 18 nM (Fig. 6A). The negative controls showed no detectable signal (Fig. 6C), which confirmed the assay is specific for detecting the interaction between LRRTM2 and NRXNα1.

For the orthogonal in-cell western assay for inhibitor hit validation, we used 0.8 µM NRXNα1-Fc as ligand for LRRTM2 interaction. We measured the inhibition of LRRTM2 and NRXNα1-Fc interaction with 300 µM AlphaScreen hit compounds, that were separately ordered for this assay. The assay shows average inhibition rate of 82% for econazole nitrate, 60% for pyrithione zinc, 54% for 6-methoxyharmalan, 54% for iodoquinol, 47% for benzoxiquine, and 46% for pyrvinium pamoate, while indole-3-carbinol did now show any inhibition. As a control, we tested for inhibition by harmaline for which the IC_{50}-value could not be determined, and it showed only 3.3 % inhibition of the signal also in the cell-binding assay (Fig. 6B). Cetylpyridinium chloride was excluded from further assays due its unlikeliness to be a specific protein binder or inhibitor based on the detergent-like structure.

4. Discussion

The presynaptic NRXNs are in particular attractive targets as they have multiple post-synaptic ligands [3], and several if not all of these proteins have been linked genetically to neuronal disorders, most probably as their misexpression will lead to synapse loss and imbalance of inhibitory/excitatory synapse-ratio and regulation of signaling in the brain. Direct studies of the effects of these proteins in neuronal culture or tissue in animal models remain quite challenging, and hence small molecule chemical probes would be highly valuable in understanding the functions of various adhesion complexes at the cellular or tissue level and in animal models.

In the current paper we establish a high-throughput method to assay for inhibitors of the synaptic NRXN-LRRTM interaction. The developed AlphaScreen-assay detecting protein-protein interaction is suitable for finding initial hits inhibiting neuronal synaptic adhesion protein interactions. Assay performs well based on statistical parameters (Table 1) highlighting the robustness and applicability

for screening of large compound libraries in singlets. The assay tolerates DMSO (up to at least 10%), enabling high compound concentrations to be screened. Here we used high compound concentrations in the validatory screening, in order to demonstrate both the performance and possibility for identifying hit compounds. High concentration of compounds challenges most screening assays through quenching the signal and affecting assay reagents. AlphaScreen assay suffers also from interference resulting in a large number of false positives in the assay setup and that makes counter-screening strategy necessary [34] . We used an Fc-His_6 construct for counter screening, and indeed found out that majority of the compounds inhibiting the signal where not inhibiting protein-protein interaction, but affected the signal by another mechanism.

In addition to counter screening it is important to measure the discovered hit effectively with an orthogonal assay. With the described cell-based assay we demonstrated that AlphaScreen assay can indeed be used to discover function compounds interfering with the LRRTM2-NRXN interaction. The assay can be readily automated for high-throughput screening and it can be also miniaturized for the high density microplates. The obtained current hit compounds have relatively low affinities based on their IC_{50}-values and are limited in their usefulness as chemical probes. Based on the orthogonal assay however, several compounds have specific inhibitory potential also in cellular environment and varied in the efficacy: while indole-3-carbinol had no effect, econazole nitrate was clearly the most promising scaffold from this compound selection in a cell-based assay (Fig. 6). Furthermore, some of the compounds active in the cell-based assay are rather small (*e.g.* benzoxiquine and 6-methoxyharmalan, Fig. 5) and could possibly be optimized for increased potency. An interesting finding is the very different effects of harmaline and 6-methoxyharmalan, which are isomers of each other, yet, harmaline (7-methoxyharmalan) was not active in the validatory assays.

The current study provides proof-of-principle for the assay and shows that it can be utilized for screening, although larger compound sets are needed to find specific high affinity binder scaffolds for further development. Together with the cell binding assay we provide a set of tools for the discovery of protein-protein interaction inhibitors. The assay was developed for LRRTM2-NRXN interaction, but could be generalizable for other adhesion proteins. This is in particular true for other NRXN-ligand interactions, *e.g.* neuroligins and LRRTMs recognize the same binding epitope on NRXNs [14, 35, 36]. Overall, to our knowledge this is the first published account on development of inhibitors towards synaptic adhesion protein interactions.

Acknowledgements

We thank the FIMM (UH) Technology Centre and Dr. Laura Turunen for help in preparing the assay plates. The use of the facilities of the Biocenter Oulu Protein Crystallography core facility and INSTRUCT-HiLIFE protein crystallization facility (UH); members of Biocenter Finland and Instruct-FI, is gratefully acknowledged. The NRXNα1 cDNA plasmid was a gift from Prof. Anne-Marie Craig and the pHYRSF53LA vector for *E.coli* expression of NRXNβ1 from Dr. Hideo Iwai. The His-tagged Fc-fragment (Fc-His_6) cloned in pETDuet-1 vector (Novagen) was obtained from Dr. Kornelia Mikula, all of which we gratefully acknowledge.

Funding

This work was funded by Jane and Aatos Erkko Foundation (TK), and Academy of Finland (grant no. 287063 and 294085 for LL).

REFERENCES

[1] G.J. Soler-Llavina, M.V. Fuccillo, J. Ko, T.C. Sudhof, R.C. Malenka, The neurexin ligands, neuroligins and leucine-rich repeat transmembrane proteins, perform convergent and divergent synaptic functions in vivo, Proc.Natl.Acad.Sci.U.S.A. 108 **(2011)** 16502-16509

[2] S. Batool, H. Raza, J. Zaidi, S. Riaz, S. Hasan, N.I. Syed, Synapse Formation: From Cellular and Molecular Mechanisms to Neurodevelopmental and Neurodegenerative Disorders, J.Neurophysiol. **(2019)**

[3] C. Reissner, F. Runkel, M. Missler, Neurexins, Genome Biol. 14 **(2013)** 213

[4] T. Südhof C., Synaptic Neurexin Complexes: A Molecular Code for the Logic of Neural Circuits, Cell 171 **(2017)** 745-769

[5] O. Gokce, T.C. Sudhof, Membrane-tethered monomeric neurexin LNS-domain triggers synapse formation, J.Neurosci. 33 **(2013)** 14617-14628

[6] M. Uchigashima, A. Cheung, J. Suh, M. Watanabe, K. Futai, Differential Expression of Neurexin Genes in the Mouse Brain, J.Comp.Neurol. **(2019)**

[7] K.A. Han, S. Jeon, J.W. Um, J. Ko, Emergent Synapse Organizers: LAR-RPTPs and Their Companions, Int.Rev.Cell.Mol.Biol. 324 **(2016)** 39-65

[8] E. Saint-Michel, G. Giannone, D. Choquet, O. Thoumine, Neurexin/neuroligin interaction kinetics characterized by counting single cell-surface attached quantum dots, Biophys.J. 97 **(2009)** 480-489

[9] C. Reissner, J. Stahn, D. Breuer, M. Klose, G. Pohlentz, M. Mormann, M. Missler, Dystroglycan binding to α-neurexin competes with neurexophilin-1 and neuroligin in the brain, The Journal of biological chemistry 289 **(2014)** 27585-27603

[10] T. Uemura, S.J. Lee, M. Yasumura, T. Takeuchi, T. Yoshida, M. Ra, R. Taguchi, K. Sakimura, M. Mishina, Trans-synaptic interaction of GluRdelta2 and Neurexin through Cbln1 mediates synapse formation in the cerebellum, Cell 141 **(2010)** 1068-1079

[11] K.L. Pettem, D. Yokomaku, L. Luo, M.W. Linhoff, T. Prasad, S.A. Connor, T.J. Siddiqui, H. Kawabe, F. Chen, L. Zhang, G. Rudenko, Y.T. Wang, N. Brose, A.M. Craig, The specific α-neurexin interactor calsyntenin-3 promotes excitatory and inhibitory synapse development, Neuron 80 **(2013)** 113; 10.1016/j.neuron.2013.07.01-128

[12] J. Ko, M.V. Fuccillo, R.C. Malenka, T.C. Sudhof, LRRTM2 functions as a neurexin ligand in promoting excitatory synapse formation, Neuron 64 **(2009)** 791-798

[13] F. Chen, V. Venugopal, B. Murray, G. Rudenko, The structure of neurexin 1alpha reveals features promoting a role as synaptic organizer, Structure 19 **(2011)** 779-789

[14] I.P. Fabrichny, P. Leone, G. Sulzenbacher, D. Comoletti, M.T. Miller, P. Taylor, Y. Bourne, P. Marchot, Structural analysis of the synaptic protein neuroligin and its beta-neurexin complex: determinants for folding and cell adhesion, Neuron 56 **(2007)** 979-991

[15] G. Rudenko, T. Nguyen, Y. Chelliah, T.C. Sudhof, J. Deisenhofer, The structure of the ligand-binding domain of neurexin Ibeta: regulation of LNS domain function by alternative splicing, Cell 99 **(1999)** 93-101

[16] J. Koehnke, X. Jin, N. Trbovic, P.S. Katsamba, J. Brasch, G. Ahlsen, P. Scheiffele, B. Honig, A.G. Palmer, L. Shapiro, Crystal structures of beta-neurexin 1 and beta-neurexin 2 ectodomains and dynamics of splice insertion sequence 4, Structure 16 **(2008)** 410-421

[17] J. Ko, G.J. Soler-Llavina, M.V. Fuccillo, R.C. Malenka, T.C. Sudhof, Neuroligins/LRRTMs prevent activity- and Ca2+/calmodulin-dependent synapse elimination in cultured neurons, J.Cell Biol. 194 **(2011)** 323-334

[18] J. de Wit, E. Sylwestrak, M.L. O'Sullivan, S. Otto, K. Tiglio, J.N. Savas, J.R. Yates 3rd, D. Comoletti, P. Taylor, A. Ghosh, LRRTM2 interacts with Neurexin1 and regulates excitatory synapse formation, Neuron 64 **(2009)** 799-806

[19] J. Lauren, M.S. Airaksinen, M. Saarma, T. Timmusk, A novel gene family encoding leucine-rich repeat transmembrane proteins differentially expressed in the nervous system, Genomics 81 **(2003)** 411-421

[20] A. Paatero, K. Rosti, A.V. Shkumatov, C. Sele, C. Brunello, K. Kysenius, P. Singha, V. Jokinen, H. Huttunen, T. Kajander, Crystal Structure of an Engineered LRRTM2 Synaptic Adhesion Molecule and a Model for Neurexin Binding, Biochemistry 55 **(2016)** 914-926

[21] A. Yamagata, S. Goto-Ito, Y. Sato, T. Shiroshima, A. Maeda, M. Watanabe, T. Saitoh, K. Maenaka, T. Terada, T. Yoshida, T. Uemura, S. Fukai, Structural insights into modulation and selectivity of transsynaptic neurexin-LRRTM interaction, Nature communications 9 **(2018)** 3964; 396-3964

[22] T.J. Siddiqui, P.K. Tari, S.A. Connor, P. Zhang, F.A. Dobie, K. She, H. Kawabe, Y.T. Wang, N. Brose, A.M. Craig, An LRRTM4-HSPG complex mediates excitatory synapse development on dentate gyrus granule cells, Neuron 79 **(2013)** 680-695

[23] P. Zhang, H. Lu, R.T. Peixoto, M.K. Pines, Y. Ge, S. Oku, T.J. Siddiqui, Y. Xie, W. Wu, S. Archer-Hartmann, K. Yoshida, K.F. Tanaka, A.R. Aricescu, P. Azadi, M.D. Gordon, B.L. Sabatini, R.O.L. Wong, A.M. Craig, Heparan Sulfate Organizes Neuronal Synapses through Neurexin Partnerships, Cell 174 **(2018)** 145-1464.e23

[24] A. Schroeder, J. de Wit, Leucine-rich repeat-containing synaptic adhesion molecules as organizers of synaptic specificity and diversity, Exp.Mol.Med. 50 **(2018)** 10

[25] I. Leshchyns'ka, V. Sytnyk, Synaptic Cell Adhesion Molecules in Alzheimer's Disease, Neural Plast. 2016 **(2016)** 6427537; 642753-6427537

[26] M. Missler, W. Zhang, A. Rohlmann, G. Kattenstroth, R.E. Hammer, K. Gottmann, T.C. Sudhof, Alpha-neurexins couple Ca2+ channels to synaptic vesicle exocytosis, Nature 423 **(2003)** 939-948

[27] T.C. Sudhof, Towards an Understanding of Synapse Formation, Neuron 100 **(2018)** 276-293

[28] L. Beaudet, J. Bedard, B. Breton, R.J. Mercuri, M.L. Budarf, Homogeneous assays for single-nucleotide polymorphism typing using AlphaScreen, Genome Res. 11 **(2001)** 600-608

[29] T.A. Bunch, Y. Grinblat, L.S. Goldstein, Characterization and use of the Drosophila metallothionein promoter in cultured Drosophila melanogaster cells, Nucleic Acids Res. 16 **(1988)** 1043-1061

[30] J.H. Zhang, T.D. Chung, K.R. Oldenburg, A Simple Statistical Parameter for Use in Evaluation and Validation of High Throughput Screening Assays, J.Biomol.Screen. 4 **(1999)** 67-73

[31] S. Bollini, J.J. Herbst, G.T. Gaughan, T.A. Verdoorn, J. Ditta, G.M. Dubowchik, A. Vinitsky, High-throughput fluorescence polarization method for identification of FKBP12 ligands, J.Biomol.Screen. 7 **(2002)** 526-530

[32] S. Karki, P. Paudel, C. Sele, A.V. Shkumatov, T. Kajander, The structure of SALM5 suggests a dimeric assembly for the presynaptic RPTP ligand recognition, Protein Eng.Des.Sel. 31 **(2018)** 147-157

[33] T. Sterling, J.J. Irwin, ZINC 15 -Ligand Discovery for Everyone, J.Chem.Inf.Model. 55 **(2015)** 2324-2337

[34] A. Yasgar, S.A. Titus, Y. Wang, C. Danchik, S. Yang, V. Vasiliou, A. Jadhav, D.J. Maloney, A. Simeonov, N.J. Martinez, A High-Content Assay Enables the Automated Screening and Identification of Small Molecules with Specific ALDH1A1-Inhibitory Activity, PloS one 12 **(2017)** e0170937

[35] D. Arac, A.A. Boucard, E. Ozkan, P. Strop, E. Newell, T.C. Sudhof, A.T. Brunger, Structures of neuroligin-1 and the neuroligin-1/neurexin-1 beta complex reveal specific protein-protein and protein-Ca2+ interactions, Neuron 56 **(2007)** 992-1003

[36] T.J. Siddiqui, R. Pancaroglu, Y. Kang, A. Rooyakkers, A.M. Craig, LRRTMs and neuroligins bind neurexins with a differential code to cooperate in glutamate synapse development, J.Neurosci. 30 **(2010)** 7495-7506

Figure Legends

Figure 1. Protein organization, interactions and the assay principle. A) Domain organization of LRRTM2 and NRXN. Main features of LRRTM2 and NRXN are indicates as: L(1-6), LNS domains 1-6; E(1-3), EGF domains 1-3; and P; PDZ binding motif. LRRTM2: white ellipsoids mark the LRR repeats 1-10, and grey ellipsoids the LRRNT and LRRCT regions. LRRTMs bind to the LNS6 domain of NRXN-α/NRXN-β. B) Schematic representation for the interaction of LRRTM2 with NRXN using the AlphaScreen assay. The interaction of LRR domain of LRRTM2 (red) with the LNS domain of NRXN (blue) brings the protein A donor beads closer to nickel chelate acceptor beads. The excitation of protein A donor beads at 680 nm convert the ambient oxygen to a excited singlet state. If an acceptor bead is within the proximity, energy is transferred from the singlet oxygen to the Acceptor bead, subsequently culminating in light production at 520-620 nm (AlphaScreen signal).

Figure 2. AlphaScreen assay development and optimization. A) The sensitivity of the AlphaScreen assay was tested with concentration series of LRRTM2-Fc and His-NRXNβ-1. The maximal signal (hook point) was determined for the assay, measured in counts per second (cps). The reaction mixture containing LRRTM2-Fc and His-NRXNβ-1were incubated for 2 hours, followed by the addition of acceptor beads and incubation for 30 minutes, after which donor beads was added with additional incubation for 60 minutes. B) The protein incubation time of LRRTM2-Fc and His-NRXN β-1 was tested for different time periods using developed AlphaScreen assay. C) The order of addition of the AlphaScreen beads was tested: (a) both beads were added together, followed by 90 min of incubation; (b) the acceptor beads were added and incubated for 30 min, followed by addition of the donor beads and addition incubation for 60 min, and (c) the donor beads were added and incubated for 30 min, followed by addition of the acceptor beads and addition incubation for 60 min. D) The optimal bead concentration was determined by incubating reaction mixture containing LRRTM2-Fc and His-NRXN β-1for 5 minutes and addition of various beads concentration and additional incubation for 90 minutes. E) The effect of bead incubation time to the signal level was optimized using a 5 µg/mL each bead concentration. F) The effect of addition of 50 nM to 5mM EGTA on the beads using the standard AlphaScreen kit (Biotinylated-HIS, PerkinElmer) G) Inhibition of NRXN-LRRTM2 interaction by EGTA at either at 2 mM (squares) or 0.2 mM Ca^{2+} (dots) concentration. In the experiment 50 nM each of LRRTM2-Fc, His-NRXNβ-1and 100 µM to 1 mM EGTA were mixed and incubated for 5 minutes before the addition of donor/acceptor beads. The results are presented as %-signal compared to the EGTA-free control. H) DMSO tolerance

assayed with reaction mixture containing 50 nM each of LRRTM2-Fc and His-NRXN β-1 and 0-10% DMSO, incubated for 5 minutes before the addition of donor and acceptor beads. The results are presented as signal percentage compare to the 0% DMSO control.

Figure 3. Primary screen results and counter screen results for identification of false positives. A) LRRTM2-Fc and His-NRXNβ-1 interaction screened against the MicroSource Spectrum compound library (%-inhibition plotted against compounds). Relative inhibition of the compounds calculated from the positive controls (0% inhibition) on the plate. The hit limit was set to >88% inhibition, based on the EGTA control (88% inhibition). B) A counter-screen experiment with the positive hit compounds from the initial screen with a Fc-His_6 protein to rule out non-specific inhibition due to interference with interaction with the beads. Compounds that showed less than 30% inhibition (dashed line) were taken forward.

Figure 4. Dose–response measurements to determine IC_{50}-values of the hit compounds. A) iodoquinol B) cetylpyridinium chloride C) benzoquinone D) pyrithione zinc E) indole-3-carbinol F) pyrvinium pamoate G) econazole nitrate H) 6-methoxyharmalan. Dose–response measurements were done with hit compounds obtained after counter screen experiment. The compounds were assayed in quadruplicates using quarter -logarithmic dilutions. Determined IC_{50}-values are given as inserts in A to H for each compound.

Figure 5. Structures of the hit compounds. Compounds are labeled A-H as in Figure 4. A) iodoquinol B) pyrithione zinc C) benzoquinone D) pyrvinium pamoate E) indole-3-carbinol F) econazole nitrate G) 6-methoxyharmalan. Molecular weight of each compounds in Daltons (Da) is included in brackets.

Figure 6. Cell-based binding assay and validation of the hit compounds with orthogonal in-cell western blot assay. A) Cell binding assay of soluble NRXNα-1-Fc (0-1000nM) to LRRTM2 on the HEK293T cells. Detected in-cell western blot signals (right) and equilibrium binding curve (left). B) Validation of the hit compounds from primary screen with the in-cell western blot assay. Detected in-cell western blot signals (right) and intensities detected in the presence of 300 µM compounds (left). Relative intensity of the assays was calculated from the positive control (100% intensity). C) Controls for the cell binding assay. From left; plain (HEK293T) cells ("-/-") , HEK293T cells with LRRTM2 transfected ("LRRTM2/ -"), plain HEK293T cells with ligand NRXNα-1-Fc added (" - /

NRXN") , HEK293T (LRRTM2 expressed) with ligand RPTPs-Fc added ("LRRTM2/RPTPσ"), and HEK293T (LRRTM2 expressed) with ligand NRXNα-1-Fc added ("LRRTM2/NRXN").

Figure 1.

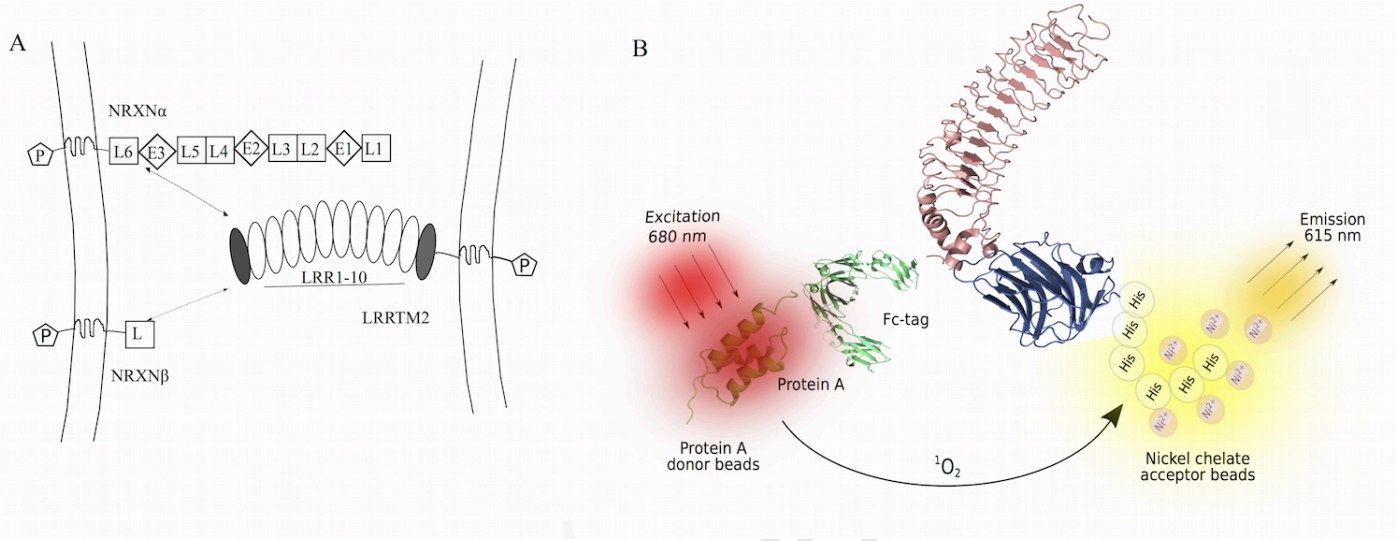

Figure 2.

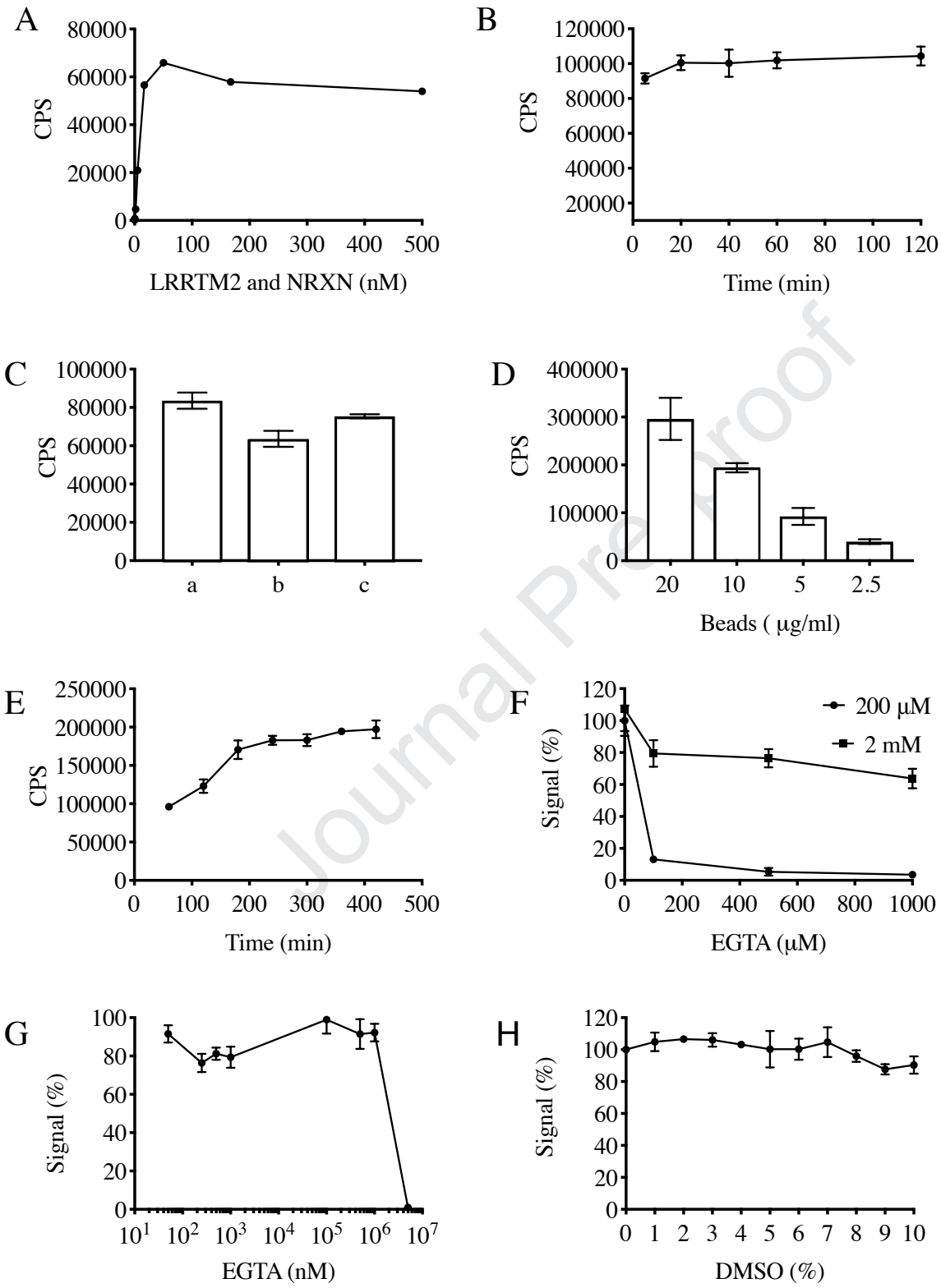

Figure 3.

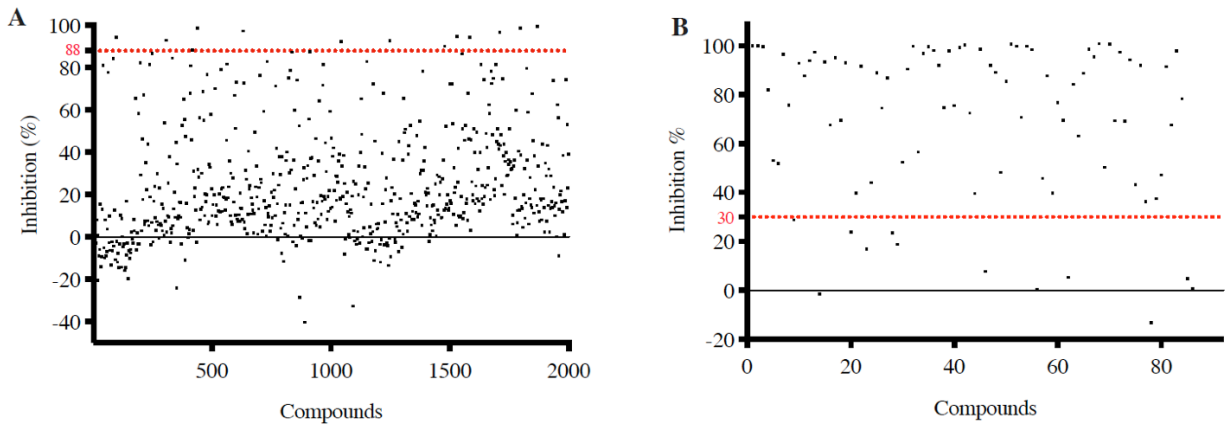

Figure 4.

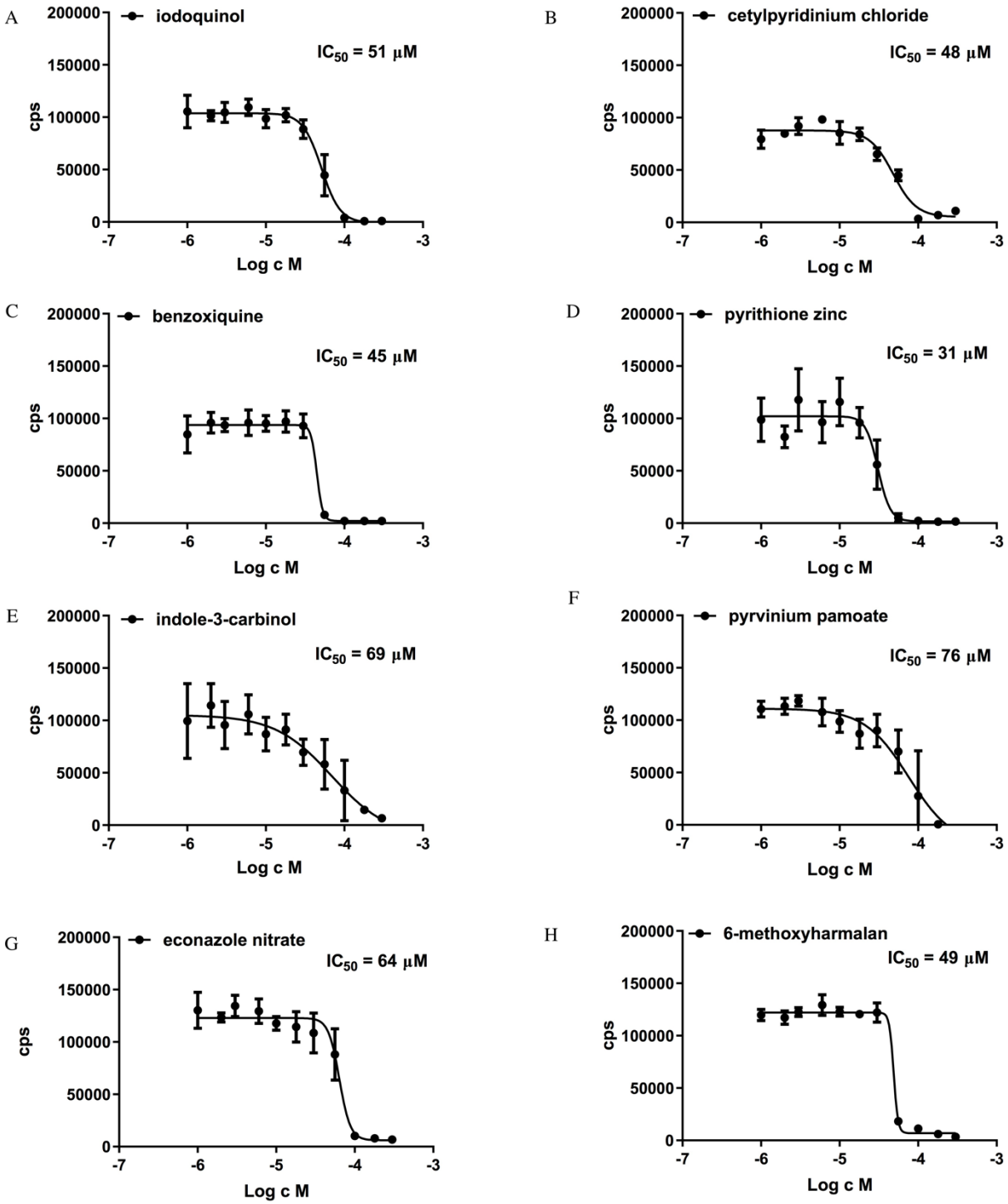
A
iodoquinol
IC50 = 51 μM
B
cetylpyridinium chloride
IC50 = 48 μM
C
benzoxiquine
IC50 = 45 μM
D
pyrithione zinc
IC50 = 31 μM
E
indole-3-carbinol
IC50 = 69 μM
F
pyrvinium pamoate
IC50 = 76 μM
G
econazole nitrate
IC50 = 64 μM
H
6-methoxyharmalan
IC50 = 49 μM
cps
Log c M

Figure 5.

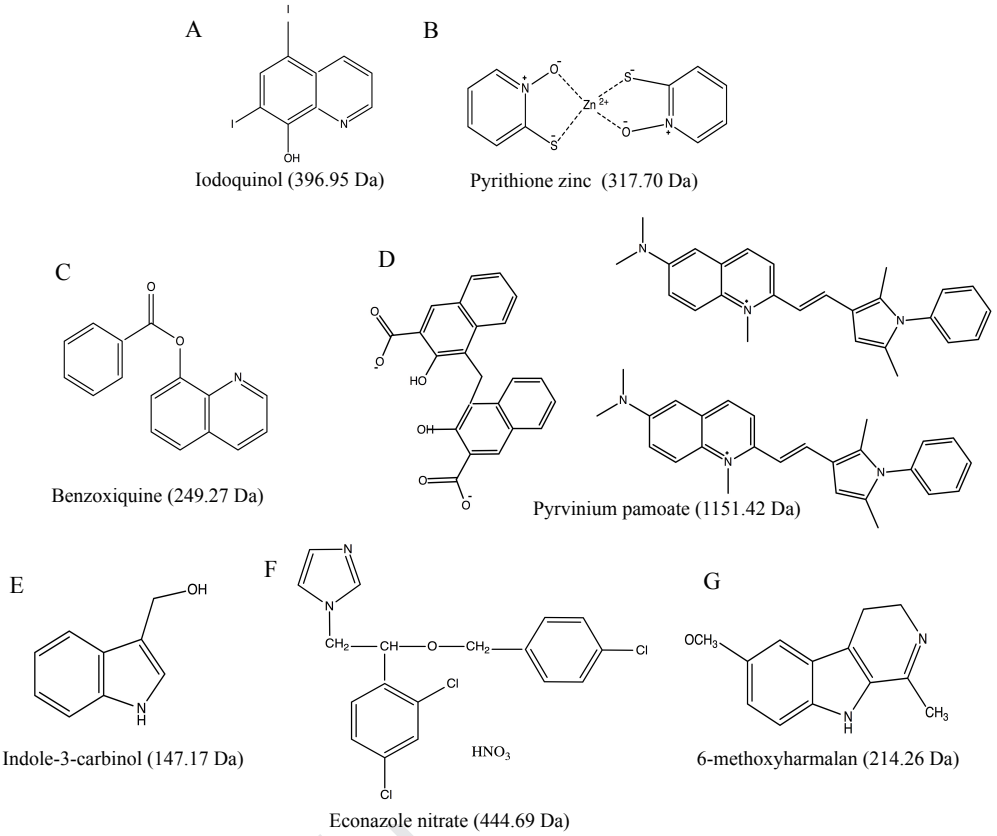

Figure 6.

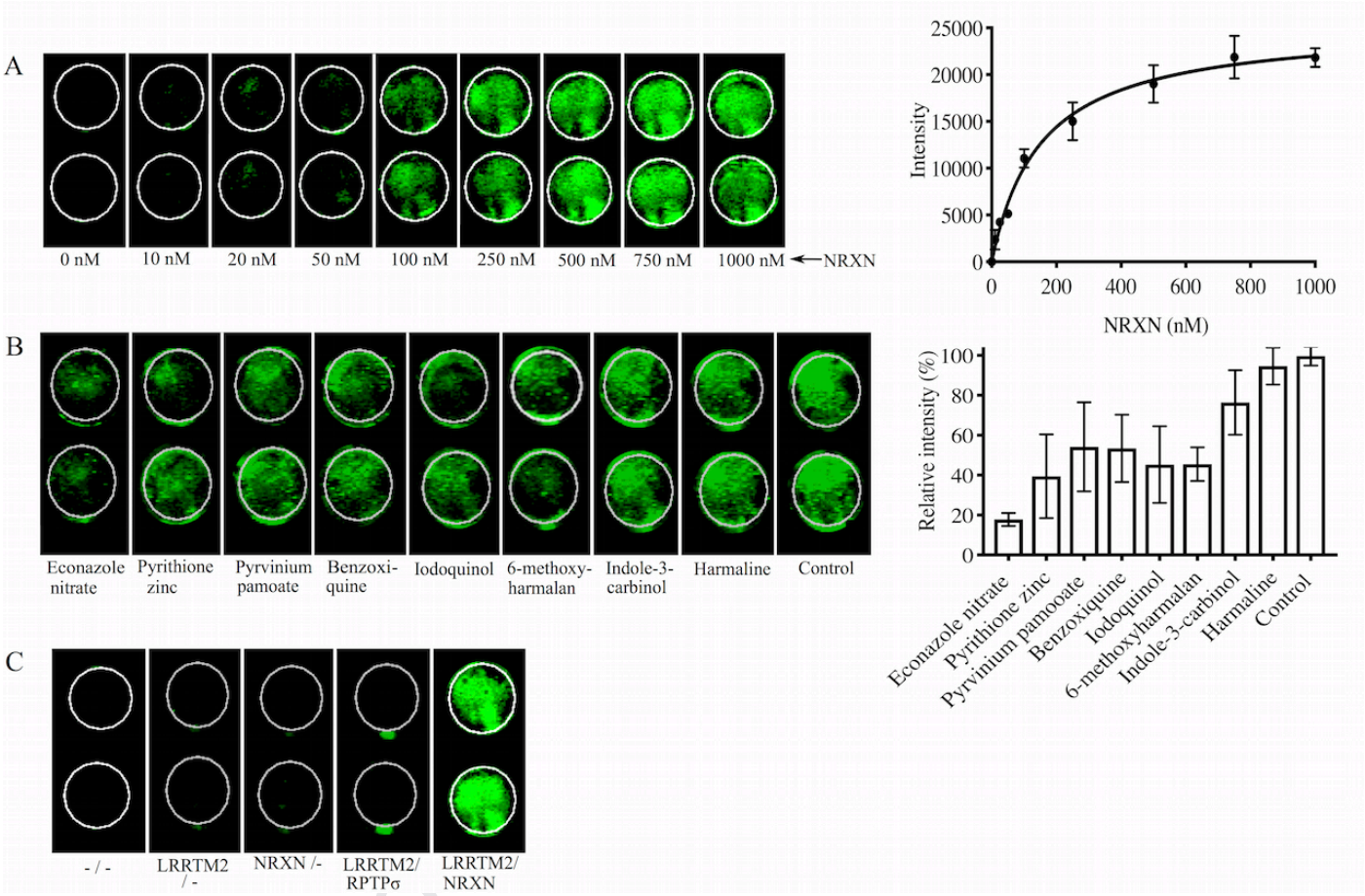
A
0 nM
10 nM
20 nM
50 nM
100 nM
250 nM
500 nM
750 nM
1000 nM
NRXN
Intensity
25000
20000
15000
10000
5000
0
0
200
400
600
800
1000
NRXN (nM)
B
Econazole nitrate
Pyrithione zinc
Pyrvinium pamoate
Benzoxi-quine
Iodoquinol
6-methoxy-harmalan
Indole-3-carbinol
Harmaline
Control
Relative intensity (%)
100
80
60
40
20
0
Econazole nitrate
Pyrithione zinc
Pyrvinium pamoate
Benzoxiquine
Iodoquinol
6-methoxyharmalan
Indole-3-carbinol
Harmaline
Control
C
- / -
LRRTM2 / -
NRXN /-
LRRTM2/ RPTPσ
LRRTM2/ NRXN

Highlights

- AlphaScreen assay for inhibitors of synaptic adhesion protein function is described
- Optimized assay was robust for screening of NRXN-LRRTM interaction inhibitors
- Eight early hit compounds were discovered
- Orthogonal cell assay is described which can be used to confirm the potency of hits